Monitoring Peak Pollution Points of Water Resources with Autonomous Surface Vehicles using a PSO-based Informative Path Planner

Micaela Jara Ten Kathen, Princy Johnson, Isabel Jurado Flores and Daniel Gutiérrez Reina

Abstract The preservation of water resources is an increasingly urgent issue. Therefore, monitoring the water quality of these resources is a very important task so that appropriate actions could be taken. This chapter focuses on water resource monitoring using a fleet of Autonomous Surface Vehicles equipped with sensors capable of measuring water quality parameters. The objective is to obtain the maximum points of contamination of the water resource through the exploration and exploitation of the water surface. The proposed algorithm is based on Particle Swarm Optimization (PSO) in combination with some machine learning techniques (Gaussian Process, Bayesian Optimization, among others) to address the limitations of PSO, such as premature convergence and difficulty in setting the initial values of the coefficients. To validate the performance of the algorithm, uni-modal and multi-modal benchmark functions are used in the simulation experiments. The results show that the proposed algorithm, the Enhanced GP-based PSO, based on the epsilon greedy method has the best performance for detecting water resource pollution peaks. It was also demonstrated that this algorithm is the one that generates the most accurate water quality model. However, when it comes to finding the highest pollution peak, the algorithm with the best response is the Enhanced GP-based PSO with a focus on exploitation.

Micaela Jara Ten Kathen
Loyola Andalucía University, Av. de las Universidades, s/n, 41704, e-mail: mcjaratenkathen@al.uloyola.es

Princy Johnson
Liverpool John Moores University, Byrom St, Liverpool L3 3AF, e-mail: p.johnson@ljmu.ac.uk

Isabel Jurado Flores
Loyola Andalucía University, Av. de las Universidades, s/n, 41704, e-mail: ijurado@uloyola.es

Daniel Gutiérrez Reina
University of Seville, C. Américo Vespucio, 41092, e-mail: dgutierrezreina@us.es

Key words: Informative Path Planning, Particle Swarm Optimization, Autonomous Surface Vehicles, Machine Learning, Water Monitoring, Multi-modal Problems

1 Introduction

Water has always been a valuable resource on the planet. However, there are major problems affecting this resource, two of which are: 1) water scarcity is increasing, and 2) human beings pollute water resources through industrial and agricultural activities, among others [7]. These problems not only affect the quality of life of human beings, but also affect the planet. One of the main consequences of water pollution by effluents can be algae blooms, which are caused by an excess of nutrients in the water (nitrates and phosphorus). This phenomenon is known as eutrophication [3]. Algae blooms are considered a major problem because they are toxic to human life and deplete oxygen from the water [2, 3]. This problem is increasingly common in the world; serious cases can be found in China, the United States, Kenya and Sri Lanka [11, 39, 22], among other places around the world.

In 2007, a massive cyanobacteria bloom in Taihu Lake, China, led to the interruption of the water supply for more than one million people [11]. It should be noted that in 1990 the lake had already suffered a similar situation, which led to the closure of 116 factories and left 3 million people without water supply [39]. A severe case of algae bloom in the United States occurred in Lake Erie in 2011. According to research [22], increased phosphorus loading in the western basin of the lake owing to agricultural operations, poor lake circulation, and meteorological conditions in the spring season that year were the main causes [22]. A case in point in Latin America is the contamination of the Ypacarai Lake, the largest lake in Paraguay (about 60 km^2). This lake has been polluted by domestic and industrial waste-water, agricultural activities, among others. As a result, the lake has an excess of nutrients, such as phosphorus and nitrates, thus promoting the appearance of cyanobacteria and affecting the population, the economy and the environment of the region [2].

Government agencies, research centers and other entities are constantly monitoring the water quality of water resources, as in the Ypacarai Lake. The traditional monitoring method consists of taking samples of the water body at specific points and analyzing these samples in laboratories. This method can be time consuming, human error can affect measurements, and costs can be high [43]. Several studies have proposed the use of intelligent vehicles for monitoring tasks [2, 25, 40]. These intelligent vehicles are surface vehicles that move autonomously, Autonomous Surface Vehicles (ASVs). The ASVs are guided by a guidance, navigation and control (GNC) system while taking water samples and measuring water quality through sensors for conductivity, nitrate, ammonium, among others. Fig. 1 shows one of the Loyola University ASVs while performing control and navigation tests at Lago de la Vida, Dos Hermanas, Spain[1].

[1] The following video shows the ASV operating at Lago de la Vida `https://www.youtube.com/watch?v=3nYzSSGeyHw`

Fig. 1: An Autonomous Surface Vehicle used for the water resource monitoring

The guidance system is in charge of determining the path that the ASVs must take. The path planners can be a global path planner [2], a local path planner [24], and an informative path planner [6]. Unlike the global and the local path planners, with the informative global path planner, the data collected by the sensors are used to generate a path based on an underlying regression model that is used to make optimal decisions. This allows to create an estimated model of the water quality parameters of the aquatic environment through machine learning (ML) techniques [6]. In this work, a meta-heuristic approach like Particle Swarm Optimization is used as a framework for developing informative path planners for monitoring tasks. The Particle Swarm Optimization (PSO) technique is one algorithm that has received a lot of attention in recent years [31, 21]. This algorithm can be used as a planner. In this piece of research, PSO is used as an informative path planner for monitoring the maximum pollution points of a water body. In addition, Gaussian Process (GP) is proposed as a surrogate model for predicting water quality parameters. GP presents important advantages for water monitoring using AVSs such as generating models with a short dataset (low number of samples) and providing the uncertainty of the generated model.

In this work, a comparison of eight PSO-based path planners is presented: the Classic PSO; the Enhanced GP-based PSO [34], using two different combinations coefficient values, [15] and [35]; 4 variants of the Enhanced GP-based PSO; and the Epsilon Greedy-based Enhanced GP-based PSO. The comparison metric used is the mean square error (MSE) between the estimated maximum pollution peaks and the actual maximum contamination points of the water resource. In addition, two more scenarios are presented: the performance of these algorithms to detect the highest pollution peak of the water resource, and to generate the most accurate model of water quality of the water resource. The main contribution of this work is the comparison of eight PSO-based path planners for monitoring maximum pollution peaks of a water resources using a fleet of autonomous surface vehicles.

The chapter layout is as follows: in Section 2, the state of the art of path planners is presented. In Section 3, the monitoring problem is explained, as well as the assumptions made to carry out the monitoring tasks. Section 4 explains the comparison of the path planners. Section 5 presents the simulation setup, experiments, and comparisons of the performances of the path planners. Section 6 provides a discussion of the results and future research directions. A conclusion of the work is presented in section 7.

2 Related Work

In recent years, the study of autonomous vehicles for the purpose of monitoring water resources has been increasing [2, 40, 26]. The monitoring is done through ASVs, equipped with sensors capable of measuring water quality parameters, which travel along the surface of the water resource taking water samples. Existing research on path planners to guide the vehicles can be found in the literature [26, 5, 25, 1]. Many path planners are based on artificial intelligence techniques that range from meta-heuristic algorithms like Genetic Algorithms (GA) [2] or Swarm-based intelligence [34], Deep Reinforcement Learning (DRL) [40], and Bayesian Optimization [26], among others.

As for meta-heuristic based approaches, the authors developed an offline path planner of an ASV in [2]. The monitoring problem was modeled as the Traveling Salesman Problem (TSP) and they used a meta-heuristic algorithm to solve it like a Genetic Algorithm (GA). In order to explore as much as possible, the authors set beacons on the lake shore. This work was extended in [1], where the monitoring problem was proposed as the Chinese Postman Problem (CPP). Unlike the TSP, with the CPP, vehicles can revisit beacons that they have previously visited, this improvement allows maximizing the coverage area to be explored. In [3], the authors proposed a two-phase approach for monitoring water resources. During the first phase, the algorithm covers the whole water body in order to find possible contaminated areas. After that, an exploitation phase is executed, where the vehicles focused on monitoring those contaminated areas found during the first stage. For both cases, the authors employed a genetic algorithm to determine the movement of an ASV. In [44], a multi-objective GA is employed for patrolling multiple water quality parameters simultaneously. The patrolling problem is different from the one proposed in this paper where the aim is to focus more frequently in those areas where higher values of contamination are found. The authors achieved Pareto-based solutions for the multi-objective problem using NSGA-II algorithm.

The path planner can also be designed using Deep Reinforcement Learning (DRL) as in [40] and Bayesian Optimization (BO) as in [26]. In [40], the authors have developed a global path planning for the monitoring of Ypacarai Lake, in which, the potential positions of the ASVs and the states are represented by RGB images of the lake. The main objective is patrolling the Ypacarai lake. A Markov Decision Problem is used to simulate the monitoring problem. The authors used a tailored reward function for training a Deep Q-learning approach based on convolutional neural networks. In [43], the authors extended the previous work, developing a multi-agent monitoring system and applied a centralized approach strategy. The authors proposed a centralized approach for training the whole fleet of ASVs with only one neural network. In addition, they demonstrated that the centralized approach is more suitable than the distributed Q-learning for the targeted patrolling problem. A comparison between Evolutionary Algorithms (EA) and DRL for monitoring systems was carried out in [42, 41]. The results showed that, in low resolution scenarios (patrolling problem), EA is more efficient. However, when the resolution of the scenario increases, DRL is more efficient. Despite requiring a greater number of hyper-parameters in the DRL than in the EA, it was shown that DRL is more suitable for problems with high complexity. In [26], the authors used the BO framework for developing an informative path planning for an ASV. The approach is focused on developing contamination maps for the Ypacarai Lake using GPs. Several tailored acquisition functions are proposed to determine the optimal locations for water quality parameter sampling. This work has been extended in [25] considering multiple water quality parameters simultaneously. The authors tested several multi-objective techniques for developing acquisition functions that fusion the information coming from several water quality parameter models to determine the optimal sample locations. A multi-agent version of this approach with region partitioning can be found in [27]. This variant allows the use of multiple ASVs to speed up the generation of contamination maps.

Regarding swarm-intelligence approaches for water monitoring, in [34], an IPP based on PSO and GP is proposed for monitoring water resources. The authors use Gaussian Processes (GP) to estimate water quality parameters. For the generation of the next points to be followed by the ASVs, the path planner uses the hyper-parameters of the PSO and the surrogate model data, uncertainty and mean. The results show that the monitoring system obtains a model very close to the real model of the water resource. The algorithm proposed by the authors, the Enhanced GP-based PSO, was compared with six other PSO-based path planners in [15] and [35]. In [15], the main goal of the monitoring system was to obtain the most accurate water quality model of the Ypacarai Lake, so the ASVs should focus on exploring the surface to achieve the goal. The results show that the Enhanced GP-based PSO, tuned with the BO, had the best performance. On the contrary, in [35], the main objective was to detect and exploit the area where the highest peak of water resource contamination was located. The algorithm that performed the best was one of the variants of the Enhanced GP-based PSO, the Contamination algorithm, where the only active term in the algorithm, apart from the velocity term, was the contamination term. In [13], the authors propose a hybrid path planning algorithm, based on Grey Wolf Optimization (GWO) and PSO, composed of 3 stages. In the first stage, the algorithm based on GWO and PSO focuses on generating and optimizing the path, smoothing the path and minimizing the path distance. The second stage, converts the infeasible points of the generated path to feasible point solutions, integrating the first stage algorithm with a Local Search technique. And the last part consists of obstacle detection and collision avoidance, using a collision avoidance algorithm. The results showed that the algorithm proposed by the authors generates short feasible paths, being an efficient path planner.

This book chapter makes a step forward with respect to previous works in terms of bench marking PSO-based algorithms for water monitoring. The proposed approach consists of comparing some PSO-based route planners in solving a multimodal problem in the area of water resources monitoring. The objective is to search for peaks of high pollution levels in a water resource. This task is carried out by eight algorithms and the performances of these algorithms are compared.

3 Statement of the problem

The monitoring challenge that the fleet of ASVs must solve, as well as the main assumptions that were used to create the simulated environment are explained in this section.

3.1 Monitoring Problem

Ypacarai Lake is the largest lake in Paraguay. This lake serves as a source of drinking water for neighboring cities, as a tourist attraction mainly in the summer season and also as a source of water for farms and crops in the surrounding area. Because of this, the contamination of the lake represents a major problem for society and for nature. The lake has two main inflows, the Pirayú stream and the Yukyry stream, and only one outflow, the Salado river, Fig. 2. The Pirayú stream is located towards the south of the lake, while the Yukury stream is located in the northwest of the lake. Other minor streams are found to the east and west of the lake shore. In addition to the lake, these streams are also often polluted [20]. Governmental and non-governmental entities conduct monitoring using the traditional monitoring method on a regular basis in order to control the pollution levels of the lake [9, 10]. Performing monitoring with ASVs will make the process more efficient and faster. As sampling with the traditional monitoring method is done at the shore of the lake, monitoring with ASVs will make it possible to detect areas of high contamination in any part of the lake, whether at the shore or in the middle of the lake.

In the monitoring system with ASVs, the water parameters are measured through water quality sensors S that are on board of the ASVs. With these measurements, the water quality model of the water body can be obtained. The function $f(\mathbf{x})$ represents the real function of the water quality model, where $\mathbf{x}$ is the position (x,y) in the water resource. The water samples are taken in an environment in a sub-space of the $\mathbb{R}^n$ space. Each ASV takes n measurements. In the vector $\mathbf{s} = \{s_k \mid k = 1, 2, \ldots, n\}$ are stored the water samples taken by the sensors, the variable k is the number of measures taken. The positions where the samples were taken are stored in $\mathbf{q} = \{q_k \mid k = 1, 2, \ldots, n\}$. The vector $D = \{(q_k, s_k) \mid k = 1, 2, \ldots, N\}$ represents the

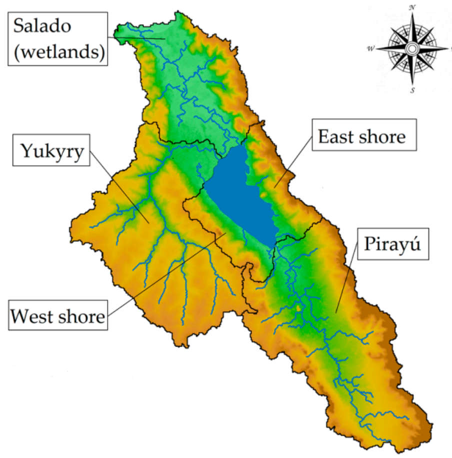

Fig. 2: Inflows and outflow of the Ypacarai Lake [20]

data acquired by the fleet of ASVs. The input of the vector D represents the position q_k of the ASVs, and the output of the vector represents the sensor data s_k. Each D_k:

$$s_k = f(q_k) \tag{1}$$

The relationship between water quality parameters y and location $\mathbf{x}$ in the Ypacarai Lake domain can be estimated by applying the regression model given by Eq. 2. Given enough data D, a real function $f(\mathbf{x})$ can be calculated.

$$y \approx f(\mathbf{x}) \tag{2}$$

3.2 Assumptions

In order to implement the proposed monitoring system, some assumptions are taken into account:

- **Ypacarai Lake:** The monitoring space model is constructed of $m \times n$ squares of side d in a matrix $\mathscr{N}$. Each element $\mathscr{N}_{i,j}$ has a value that represents the current state of the grids, 0 (white) indicates forbidden zone, land, among others, and 1 (black) indicates the zone where the ASVs can travel. Fig. 3 shows the occupation grid of Ypacarai Lake. For simulations, the distribution map was scaled, each element $\mathscr{N}_{ij}$ is 100 m $\times$ 100 m.
- **Coordinator**: A centralized system is used for control and communication between the ASVs. To this end, the ASV fleet is connected to a global coordinator via the cloud, using 4G or 5G technology. To avoid jams and bumps, a safety

zone is considered on the lake shore, so ASVs are not allowed to travel too close to the lake shores.

- **Sensors:** The measurements made by the sensors are error-free. In addition, the position estimated by the GPS of the ASVs is free of noise.
- **Navigation:** The movements of the ASVs are flawless. Because of this, the trajectories of the ASVs are completely accurate. Obstacles and collisions are not considered. The speed limit for the ASVs is 2 m/s.
- **Vehicle autonomy:** Battery consumption is acceptable for the duration of the tests. The ASVs can reach a maximum distance of about 15,000 metres.

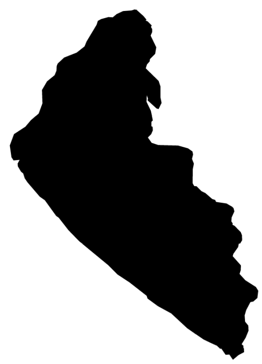

Fig. 3: Model of the occupancy grid of the Ypacarai Lake

4 PSO-based path planning algorithms

This section presents the informative path planners considered for the proposed comparison.

4.1 Classic Particle Swarm Optimization (PSO)

The PSO algorithm was developed by the authors in [16] using the social behavior of birds flocking as inspiration. PSO is a heuristic optimization algorithm in which each individual (particle) is a potential solution of the optimization problem. The particle has a position, which represents a possible solution, and a velocity, which determines the distance and direction each particle must travel. The velocity of the particle is updated according to the best position found by each particle (local best) and the best position found by all the particles in the swarm (global best) during the search process. The position of the particle is updated according the velocity. The velocity $\mathbf{v}_p^{t+1}$ and the position $\mathbf{x}_p^{t+1}$ of the pth particle at time step t, t represents discrete time steps, are described as follows:

$$\mathbf{v}_p^{t+1} = w\mathbf{v}_p^t + c_1 r_1^t \left[\mathbf{pbest}_p^t - \mathbf{x}_p^t\right] + c_2 r_2^t \left[\mathbf{gbest}^t - \mathbf{x}_p^t\right] \tag{3a}$$
$$\mathbf{x}_p^{t+1} = \mathbf{x}_p^t + \mathbf{v}_p^{t+1} \tag{3b}$$

where w represents the inertia weighting, $\mathbf{pbest}_p^t$ is the local best of the particle and $\mathbf{gbest}^t$ is the global best of the swarm. These two terms refer to the exploitation and exploration of the search space respectively. The constants c_1 and c_2 are acceleration coefficients that describe the relative relevance of the local best and global best. r_1 and r_2 are random numbers in the interval [0, 1]. Notice that in the proposed monitoring system each particle will represent an ASV. Thus, the movements of the ASV will be influenced by the maximum level of contamination sensed by an ASV of the fleet $\mathbf{gbest}^t$ and its local maximum level, that is, the maximum contamination level sensed by an ASV so far $\mathbf{pbest}_p^t$.

4.2 Enhanced GP-based PSO

This subsection is divided into four parts. The first part explains the surrogate model that is used to guide the vehicles to the positions of maximum uncertainty and zones of maximum contamination level of the water resource. The second part explains how the path planner itself works. In the third part, the BO, which is the technique selected for the optimization of the hyper-parameters, is described. Finally, the four variants of the Enhanced GP-based PSO that are also compared with the other path planners are described.

4.2.1 Gaussian Process Regression (GPR)

GP are Bayesian inference-based probabilistic machine learning models [28]. The input is constructed as a multivariate normal distribution. Each data of the input represents a random variable. The GP is completely defined by its mean function and covariance (or kernel) function [28]. However, the mean function is usually considered to be zero. Therefore, the component that defines the behavior of the GP is the kernel function. In the path planner to be analyzed, the kernel function plays the role of specifying the expected variability, smoothness and shape of the water quality parameters to be monitored. Taking into account the results of [26], the kernel function used for the experiments is the Radial Basis Function (RBF), because it is the most suitable for water resources.

The input data D is marginalized and conditioned to update the GPR [36]. For the computation of the unknown response $(\mu(\mathbf{x}_*), \sigma(\mathbf{x}_*))$ of the GPR $(\hat{f}(\mathbf{x})_*)$, the following set of Eq. 4 is used:

$$\mu_{\hat{f}(\mathbf{x}_i)_*|D} = K_*^T K^{-1} f(\mathbf{x}) \tag{4a}$$

$$\sigma_{\hat{f}(\mathbf{x}_i)_*|D} = K_{**} - K_*^T K^{-1} K_* \tag{4b}$$

where K, K_{**} and K_* are extracted from the fitted kernel, which includes covariances between known data $k(\mathbf{x},\mathbf{x})$ and unknown data $k(\mathbf{x}*,\mathbf{x}*)$, as well as covariances between both the known and unknown data $k(\mathbf{x},\mathbf{x}*)$.

$$K = \begin{bmatrix} K & K_* \\ K_*^T & K_{**} \end{bmatrix} = \begin{bmatrix} k(\mathbf{x},\mathbf{x}) & k(\mathbf{x},\mathbf{x}*) \\ k(\mathbf{x}*,\mathbf{x}) & k(\mathbf{x}*,\mathbf{x}*) \end{bmatrix} \tag{5}$$

4.2.2 Path Planner

Aiming to overcome the limitations of the Classic PSO, research in [34] developed an informative path planner based on PSO and GP (as a surrogate model). The two components of the GP are considered in the path planner, the covariance or kernel function (σ) and the mean function (μ). The kernel function is considered to guide the ASVs to areas of the water body that have not yet been explored, and the mean function is used for the purpose of exploiting areas where water resource contamination levels are high. The ASV velocity is updated according to Eq. 6 and the position is updated according to Eq. 3b.

$$\begin{aligned}\mathbf{v}_p^{t+1} = {} & w\mathbf{v}_p^t + c_1 r_1^t[\mathbf{pbest}_p^t - \mathbf{x}_p^t] + c_2 r_2^t[\mathbf{gbest}^t - \mathbf{x}_p^t] + c_3 r_3^t[\mathbf{max\_un}^t - \mathbf{x}_p^t] + \\ & c_4 r_4^t[\mathbf{max\_con}^t - \mathbf{x}_p^t]\end{aligned} \tag{6}$$

where the coordinate of the maximum value of the uncertainty of the surrogate model uncertainty $max\sigma^t$ at tth iteration is represented by $\mathbf{max\_un}^t$ and the coordinate of the maximum value of the mean (or contamination) $max\mu^t$ of the surrogate model at tth iteration is represented by $\mathbf{max\_con}$. The constants c_3 and c_4, as well as c_1 and c_2, are acceleration coefficients that determine the importance of exploration (uncertainty) and exploitation (mean or contamination). These four acceleration coefficients must be tuned after starting the monitoring task.

The water sample is taken after traveling a distance of l between the current ASV position ($\mathbf{x}^t$) and the last position where a sample was taken ($\mathbf{x}_{sample}$). The distance l is calculated by applying the Eq. 7:

$$l = \lambda \times \ell^t \tag{7}$$

where the term λ represents a ratio of the different length scales, and the ℓ^t refers to the posterior length scale of the surrogate model [25]. By applying this condition, the ASVs take samples at specific points, increasing the speed of execution of the monitoring system.

Fig. 4 shows the flowchart of the path planner based on PSO and GP. At the beginning, the coordinates of the maximum uncertainty and maximum contamination are equal to 0. As a result, until the first sample is taken, the behavior of the path planner is the same as the Classic PSO. A water sample is taken after the ASV travels a minimum distance l. With these data, the GP is updated. Then, the coordinates of the maximum uncertainty and contamination values are found to update the ASV velocity and position.

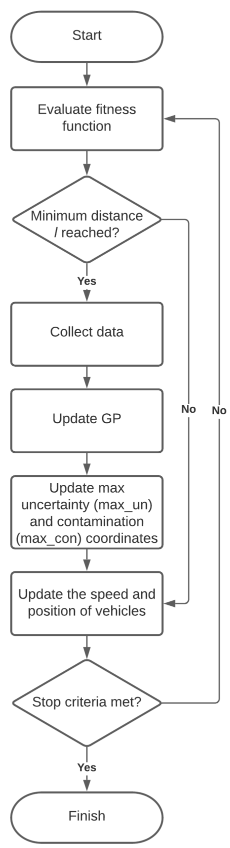

Fig. 4: Flowchart of the Enhanced GP-based PSO

4.2.3 Hyper-Parameter Optimization

In order for the navigation system to behave correctly, the acceleration coefficients, c_1, c_2, c_3 and c_4, must be tuned. Hyper-parameter optimization techniques range from meta-heuristic algorithms to neural networks [4, 19, 14]. These techniques allow to obtain a better performance of the algorithms with reduced human effort [12]. The selected technique to tune the Enhanced GP-based PSO coefficients is the BO.

BO is a very successful optimization technique for solving tuning tasks, and it may be used in functions that are difficult to calculate, functions with a significant difficulty in analyzing their derivatives, and non-convex functions [37]. The procedure applies the Bayes theorem, Eq. 8, to integrate previous information about the unknown function with data information, G, to obtain the posterior of the function:

$$P(F|G) = P(G|F) \times P(F) \tag{8}$$

where $P(F|G)$ refers to the posterior probability of the model F; given model F, $P(G|F)$ represents the likelihood of overserving G; and $P(F)$ refers to the previous probability.

BO optimises a function using a surrogate model that is updated according to the information provided by the evaluated points [30]. The acquisition function, such as Probability of improvement (PI) [18], Expected improvement (EI) [23], GP upper confidence bound (GP-UCB) [33], is used to balance exploration and exploitation in the selection of the next location to explore. Readers are referred to [30, 17, 37] for a full examination of BO-based hyper-parameter optimization. The results obtained in [37] indicate that the PI function is slower than the EI and GP-UCB functions, and that GP-UCB is more complicated than EI because in the GP-UCB function hyper-parameters must be tuned. Because of this, EI has been selected as the acquisition function of the BO.

4.2.4 Variants of the Enhanced GP-based PSO

These variants consist of keeping the velocity term and one of the exploration and exploitation term from Eq. 3a. The main objective is to evaluate the performance of the Enhanced GP-based PSO when only one of these terms is considered. The variants are as follows:

- **Local Best:** the active term in this algorithm is the local best $\mathbf{pbest}_p^t$ term. As a result, the trajectory generated by the algorithm is guided by the best position reached so far by the ASV. Since only the local best is considered, this algorithm focuses on the exploitation considering the zones where the ASV has already traveled. The velocity is updated according to Eq. 9:

$$\mathbf{v}_p^{t+1} = w\mathbf{v}_p^t + c_1 r_1^t [\mathbf{pbest}_p^t - \mathbf{x}_p^t] \tag{9}$$

- **Global Best:** in this algorithm the best position of the swarm found so far, the global best $\mathbf{gbest}^t$, is considered. The ASVs learn from the swarm experience and focus on surface exploration. The equation used for updating the velocity of the ASVs is shown below:

$$\mathbf{v}_p^{t+1} = w\mathbf{v}_p^t + c_2 r_2^t [\mathbf{gbest}^t - \mathbf{x}_p^t] \tag{10}$$

- **Uncertainty:** unlike the first two variants that consider the experience of the ASVs, this algorithm considers the data obtained from the surrogate model. This is because the term that remains active is the uncertainty of the model **max_un**. Because of this, the algorithm focuses on the exploration of unexplored areas. The velocity of the ASVs are updated according to Eq. 11:

$$\mathbf{v}_p^{t+1} = w\mathbf{v}_p^t + c_3 r_3^t [\mathbf{max\_un}^t - \mathbf{x}_p^t] \tag{11}$$

- **Contamination:** as the uncertainty algorithm, this algorithm considers the data obtained from the surrogate model, the mean of the model **max_con**. This allows the algorithm to focus on the exploitation of the areas with the highest levels of water resource contamination. The velocity of the ASVs is updated according to Eq. 12:

$$\mathbf{v}_p^{t+1} = w\mathbf{v}_p^t + c_4 r_4^t [\mathbf{max\_con}^t - \mathbf{x}_p^t] \tag{12}$$

The position of the ASVs in all variants of the algorithm is updated according to Eq. 3b.

4.3 Enhanced GP-based PSO based on Epsilon Greedy Method

The epsilon greedy method allows the PSO-based path planner to have dynamic coefficients. With dynamic coefficients, the enhanced GP-based PSO can balance exploration and exploitation by randomly choosing between the two. As a result, the path planner will be switching between exploration and exploitation phases.

Algorithm 1 shows the pseudocode of the Epsilon Greedy method. The value of the epsilon function has three parts. First, the epsilon function ε has a high value, 0.95. This means that the probability of exploring unknown areas is 95%. Once an ASV reaches a traveled distance $d\varepsilon_0$, the epsilon greedy moves to the second part. In this second part, the value of the epsilon function ε decreases $\Delta\varepsilon$ as the ASVs travel approximately 1,000 meters. When an ASV reaches a traveled distance $d\varepsilon_f$, the value of the epsilon function ε is fixed at 0.05; this is the third part. In other words, the ASVs have a 5% of probability of exploring unknown areas and a 95% of probability of exploiting areas with high levels of contamination. After every 1,000 meters traveled by the ASVs, a random number *val* is obtained and compared to the epsilon function ε. If the random number *val* is less than the epsilon function ε, the ASV's focus is exploring (*Explore*) the surface water resource, and if the random number *val* is greater than the epsilon function ε, the ASV's focus is exploiting (*Exploit*) areas with high levels of contamination. The behavior of the path planner is the same as that the Enhanced GP-based PSO (Section 4.2) once the coefficient values are defined.

Algorithm 1: Enhanced GP-based PSO based on Epsilon Greedy method pseudo-code

```
x_p^0 ← Initialize PSO; // where x^0 represents the initial position of p
while not done do
    if dist_total ≤ dε_0 then
        ε^t ← 0.95
    else if dist_total ≥ dε_f then
        ε^t ← 0.05
    else
        ε^t ← ε^{t-1} − Δε
    val ← random();
    if ε^t ≥ val then
        c_1, c_2, c_3, c_4 ← Explore
    else
        c_1, c_2, c_3, c_4 ← Exploit
    pbest_p, gbest ← Evaluate fitness function;
    dist ← dist_total − dist_sample ← Calculate distance;
    if dist ≥ l then
        s ← Collect sensor data;
        σ^t, μ^t ← Update GP;
        maxσ^t, maxμ^t ← Calculate maximum values;
        max_un^t, max_con^t ← Find coordinates of the maximum values;
    v_p^{t+1}, x_p^{t+1} ← Update speed and position of the particles;
```

In Algorithm 1, the average distance traveled by an ASV, p, between the current position and the initial position is represented by the term $dist_{\text{total}}$ and the average distance traveled by an ASV between the current position and the position where the last sample was taken is represented by $dist_{\text{sample}}$.

5 Results

This section presents the obtained simulations results. First, the ground truth function used as water quality parameter model is described. Second, the performance metric used to compare the algorithms is mentioned. Third, the simulation parameters used for the comparison are detailed. Next, the results of the hyper-parametrization carried out for the PSO-based algorithms are shown. Finally, the performance comparison of the algorithms is presented.

The path planners were developed in Python and the following libraries were used: Scikit-learn[2] (accessed on 5 May 2022), DEAP[3] (accessed on 5 May 2022) and Bayesian Optimization[4] (accessed on 5 May 2022).

5.1 Ground Truth

As ground truth a scaled model of the Ypacarai Lake is used, each element has a dimension of 100 m x 100 m. A benchmark function, the Shekel function (Eq. 13), is used as a distribution map of water quality parameters. This function is used because it is a multidimensional, multimodal, deterministic, and continuous function [25].

$$f_{\text{Shekel}}(\mathbf{x}) = \sum_{i=1}^{M} \frac{1}{c_i + \sum_{j=1}^{N} (x_j - a_{ij})^2} \tag{13}$$

The function allows specifying multiple maximum points by means of two arguments, a_{ij} and c_{ij}. The element a_{ij} belongs to the matrix A. This matrix has a size of $M \times N$, M corresponds to the number of maximum points and N to the dimensions of the space. The matrix C, whose elements are c_{ij} and whose size is $M \times 1$, defines the inverse significance value of the maximum positions. Ten different ground truths are used to analyze the behavior of path planners. Since the objective is to detect several contamination peaks, the value of M varies between 2 and 4. These peaks are located near the flow inlets of Ypacarai Lake, the location and number of peaks are randomly selected. The value of N is fixed at 2. The values of the elements of c are random numbers. Fig. 5 shows an example of ground truth used in the simulations. It is possible that the peaks are located in prohibited areas.

5.2 Performance metric

The mean squared error (MSE) is used as a comparison metric to evaluate the performance of the path planners for two of the situations presented in this work, the main objective being the detection of several peaks of water resource contamination, and for obtaining the most accurate model of the water quality of the water resource. The MSE is often used to evaluate regression models. This is the reason for the selection of this metric as an evaluation method. The Eq. 14 represents the MSE between the real model or ground truth ($f(\mathbf{x})$) and the estimated model or

[2] https://scikit-learn.org/stable/

[3] https://deap.readthedocs.io/en/master/

[4] https://github.com/fmfn/BayesianOptimization

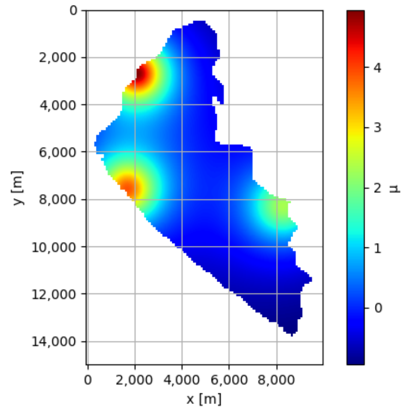

Fig. 5: Example of one of the ten ground truth obtained with the Shekel function used for the simulations of the monitoring system in Ypacarai Lake.

the resulting prediction (y) of the surrogate model to compare the peaks of water resource contamination.

$$\mathrm{MSE}_{peaks}(f(\mathbf{x}),y) = \frac{1}{n_{peaks\_points}} \sum_{k=0}^{n_{peaks\_points}-1} (f(\mathbf{x}_k) - y_k)^2 \tag{14}$$

The main objective is to detect the points of maximum contamination of the water body. Therefore, the MSE between the contamination peaks of the real model or ground truth and the contamination peaks of the estimated model is calculated. As a result, the path planner with the best MSE (low MSE) is considered the optimal path. Then, to obtain the most accurate model of the water quality of the water resources, the MSE between all the coordinates of the actual model and the estimated model is calculated. The Eq. 16 represents the MSE between the real model or ground truth ($f(\mathbf{x})$) and the estimated model or the resulting prediction (y) of the surrogate model to compare the water quality model of the lake.

$$\mathrm{MSE}_{map}(f(\mathbf{x}),y) = \frac{1}{n_{map\_points}} \sum_{k=0}^{n_{map\_points}-1} (f(\mathbf{x}_k) - y_k)^2 \tag{15}$$

Another situation is to detect the highest peak pollution of the water resource. To evaluate the performance of the path planners, the error between maximum ground truth peak pollution and the maximum pollution peak of the estimated model is calculated. The Eq. 16 represents the error between the real model or ground truth ($f(\mathbf{x})$) and the estimated model or the resulting prediction (y) of the surrogate model to compare the highest contamination peak of the water resource.

$$\mathrm{Error}_{highest\_peak}(f(\mathbf{x}),y) = |f(\mathbf{x}_{highest\_peak}) - y_{highest\_peak}| \tag{16}$$

5.3 Setting Simulation Parameters

This subsection presents the general settings of the simulations. In addition, the results of the hyper-parametrization carried out for the PSO-based algorithms are shown.

5.3.1 Global simulation parameters

The mission will be carried out using four ASVs. Each ASV covers around 15,000 metres and travels at a top speed of 2 metres per second. The inertia is set to a value of one. In order for the length scale to provide the necessary smoothness, the value should be set to 10% of the length of the search space [26]. Therefore, the value of the length scale is set to 10. The value of λ is set on 0.3. With this value, the ASVs take around 120 samples. The stopping criteria of the path planners is the distance traveled by the ASVs, when an ASV has traveled 15,000 meters, the simulation ends.

5.3.2 Results of hyper-parametrization of Enhanced GP-based PSO

In this work, two cases of the Enhanced GP-based PSO have been considered, [15] and [35]. The difference between these cases is the main objective of the monitoring task. Because of this, the combination of the coefficient values are different in both cases. The hyper-parametrization of each case is presented below.

5.3.2.1 Enhanced GP-based PSO (Exploration)

For the hyper-parametrization presented in [15], the main idea was to obtain the most accurate water quality model. As a consequences, the algorithm focus on the exploration of the water resources surface. Two cases were considered for the hyper-parametrization. In the first case, 200 ground truth were evaluated for the BO. In the second case, the number of ground truth evaluated was 300. For both cases BO will be used for hyper-parameter optimization, with the selected acquisition function being EI. The kernel function used for hyper-parameter optimization was the default function of the Bayesian-Optimization library, Matérn, with parameter values equal to $nu = 2.5$ and $\ell = 1.0$. The number of BO iterations was set to 20, and 10 random starting points were considered.

Table 1: Range for hyper-parameter optimization

Hyper-parameter	Range
c_1	[0, 4]
c_2	[0, 4]
c_3	[0, 4]
c_4	[0, 4]

The range of the PSO hyper-parameters (coefficient acceleration of the local best, c_1; coefficient acceleration of the global best, c_2; coefficient acceleration of the maximum uncertainty, c_3; and coefficient acceleration of the maximum contamination, c_4) is determined according to [29, 32], Table 1. Table 2 shows the results obtained in each case of hyper-parameter optimization for the exploration approach.

Table 2: Hyper-parameter values in each case of the BO for the Enhanced GP-based PSO (Exploration)

Hyper-parameter	Case 1 200 Ground Truth	Case 2 300 Ground Truth
c_1	2.0187	3.0970
c_2	0	0.0125
c_3	3.2697	3.5863
c_4	0	0.0382

The comparison between the MSE results obtained from the monitoring system performance of each case is shown in Table 3. The MSE values are very similar, the difference is 0.003. This is because the values of the coefficients obtained in both optimization cases do not differ much, with c_3 being the dominant coefficient, and c_2 and c_4 being 0 or practically 0. In other words, the monitoring system is driven by the maximum uncertainty of the model and by the best local of each particle. The values of the coefficients for comparison with the other methods will be the values of Case 1, since it has the best MSE.

Table 3: Comparison of the MSE of the BO cases for the Enhanced GP-based PSO (Exploration)

Case	MSE
1	**0.02650** $\pm$ **0.02727**
2	0.02916 $\pm$ 0.02952

5.3.2.2 Enhanced GP-based PSO (Exploitation)

Unlike the work presented in [15], the hyper-parameterization objective presented in [35] was to find the highest contamination peak. Because of this, the focus of the algorithm was to exploit the areas of high contamination level. The cases considered in this work were the same as the cases presented in Section 5.3.2.1. Since the objective of this work was to obtain the highest contamination peak, the comparison metric used was the error committed between the actual value of the peak and the estimated value of that peak. In the first case, the mean of the error of 200 ground truth was considered for the BO, and for the second case, 300 ground truth was considered. The configurations of the acquisition function, the kernel function and the BO used were also the same as the configurations presented in Section 5.3.2.1. Also, the ranges of the coefficients used for the hyper-parametrization are the same as those presented in the Table 1. Table 4 shows the results obtained in each case of hyper-parameter optimization for the exploitation approach.

Table 4: Hyper-parameter values in each case of the BO for the Enhanced GP-based PSO (Exploitation)

Hyper-parameter	Case 1 200 Ground Truth	Case 2 300 Ground Truth
c_1	0.5683	3.6845
c_2	3.4160	1.5614
c_3	0	0
c_4	3.1262	3.6703

The comparison of the errors made between the actual value of the peak and the value estimated by the algorithm are presented in Table 5. The difference between the error values is less that 0.003. The main difference between the two cases is the values of the local and global best coefficients. While in case 1, the value of local best is low and global best is high, in case 2 local best has a higher value than global best. This means that in case 2, the exploitation of the area is more intensive since the local best and maximum contamination terms allow the algorithm to perform the exploitation.

Table 5: Comparison of the MSE of the BO cases for the Enhanced GP-based PSO (Exploitation)

Case	Error
1	0.00818 ± 0.03139
2	**0.00540 ± 0.01399**

5.3.3 Setting Epsilon Greedy Method

Before making the comparison between the algorithms, four cases of the epsilon greedy method have been compared. In two cases, the values of the coefficients for the exploration stage are: $Explore$: $c_{1explore} = 1$, $c_{2explore} = 4$, $c_{3explore} = 4$, $c_{4explore} = 1$; and for exploitation stage are: $Exploit$: $c_{1exploit} = 4$, $c_{2exploit} = 1$, $c_{3exploit} = 1$, $c_{4exploit} = 4$. The values of the coefficients are determined according to the range given in [29, 32]. For the other two cases, the values for the exploration are the values obtained from the BO in the paper [15]: $Explore$: $c_{1explore} = 2.0187$, $c_{2explore} = 0$, $c_{3explore} = 3.2697$, $c_{4explore} = 0$, and for the exploitation stage, the values are the values obtained from the BO in the paper[35]: $Exploit$: $c_{1exploit} = 3.6845$, $c_{2exploit} = 1.5614$, $c_{3exploit} = 0$, $c_{4exploit} = 3.1262$. The values for the cases are shown in Table 6.

Table 6: Parameter and hyper-parameter values in each case of the Epsilon Greedy method

Parameter/Hyper-parameter	Case 1	Case 2	Case 3	Case 4
$d\varepsilon_0$ (m)	5,000	3,000	5,000	3,000
$d\varepsilon_f$ (m)	10,000	12,000	10,000	12,000
$\Delta\varepsilon$	0.18	0.116	0.18	0.116
$c_{1explore}$	1	1	2.0187	2.0187
$c_{2explore}$	4	4	0	0
$c_{3explore}$	4	4	3.2697	3.2697
$c_{4explore}$	1	1	0	0
$c_{1exploit}$	4	4	3.6845	3.6845
$c_{2exploit}$	1	1	1.5614	1.5614
$c_{3exploit}$	1	1	0	0
$c_{4exploit}$	4	4	3.1262	3.1262

Since the vehicles travel approximately 15,000 meters each, for the cases 1 and 3, the values of $d\varepsilon_0$ and $d\varepsilon_f$ were set by dividing the total distance into three equal parts, 5,000 and 10,000 meters respectively. For the second part of the algorithm, the value of ε decreases by 0.18 every 1,000 meters traveled. For the cases 2 and 4, the distance was increased for the second part, the values of $d\varepsilon_0$ and $d\varepsilon_f$ are 3,000 and 12,000 meters, respectively, and the value of ε decreases by 0.116 every 1,000 meters traveled.

In addition to detecting all contamination peaks of the Ypacarai Lake (multi-modal problem), two other situations were considered: detecting the highest contamination peak (uni-modal problem), and creating the most accurate model of the lake. The MSE values for all cases and situations are shown in Table 7. For the uni-modal problem, the error between the actual value and the estimated value of the peak was calculate.

Table 7: Comparison of the MSE and error of the Epsilon Greedy cases

Case	MSE (Several Contamination Peaks)	Error (A Contamination Peak)	MSE (Model of the Lake)
1	**1.62302 $\pm$ 4.32203**	1.18271 $\pm$ 3.48666	0.07334 $\pm$ 0.12163
2	1.71359 $\pm$ 4.56390	1.27596 $\pm$ 3.63597	0.07645 $\pm$ 0.13131
3	**1.62643 $\pm$ 3.64945**	**0.00984 $\pm$ 0.03666**	**0.07018 $\pm$ 0.10068**
4	1.65896 $\pm$ 4.30441	0.33264 $\pm$ 1.67548	0.07327 $\pm$ 0.12753

The case with the best MSE for detecting all the peaks in the lake map was obtained with case 1, where the values of the coefficients were 1 and 4. However, case 3 also obtained a good MSE, with a difference of about 0.004 with respect to case 1, and it also has the smallest range of variability. As for the situation where there is only one contamination peak, the best MSE is in case 3. Likewise, when the objective is to obtain the most accurate model of the lake, case 3 has the best MSE. Therefore, the coefficient values of case 3 are selected for comparison with the other algorithms.

5.4 Performance Comparison

After selecting the best configuration of PSO-based algorithms, comparisons are made with the other algorithms. The values selected for the Epsilon Greedy method are the values of case 3. These results are compared with the Classical PSO, the Enhanced GP-based PSO using the values obtained from the [15] and [35] papers (described in previous subsections), and with the four variants of the Enhanced GP-based PSO. The Table 8 and Table 9 show the values of the coefficients for each algorithm. [38, 8] were considered to determine the coefficient values for the Classic PSO. Since the objective is to observe the influence of the terms, for the Local Best, Global Best, Uncertainty and Contamination algorithms was decided not to set the maximum value of the range.

Table 8: Acceleration coefficients values

Hyper-parameter	Local Best Algorithm	Global Best Algorithm	Uncertainty Algorithm	Contamination Algorithm	Classic PSO	Enhanced GP-based PSO (Exploration)	Enhanced GP-based PSO (Exploitation)
c_1	3	0	0	0	2	2.0187	3.6845
c_2	0	3	0	0	2	0	1.5614
c_3	0	0	3	0	0	3.2697	0
c_4	0	0	0	3	0	0	3.1262

Table 9: Acceleration coefficients values for the Epsilon Greedy method

Hyper-parameter	Value
$c_{1explore}$	2.0187
$c_{2explore}$	0
$c_{3explore}$	3.2697
$c_{4explore}$	0
$c_{1exploit}$	3.6845
$c_{2exploit}$	1.5614
$c_{3exploit}$	0
$c_{4exploit}$	3.1262

For the experiments, the following considerations were taken into account: a) each vehicle starts from a different starting point than the others, however, in all simulations, each vehicle starts from the same initial position; b) the error and MSE calculations are performed considering 10 different scenarios; c) the water sample is taken after the vehicles have traveled a distance l (Eq. 7); and d) the simulation ends when one of the vehicles travels 15,000 meters.

The best performing algorithm for detecting contamination peaks is the Enhanced GP-based PSO based on Epsilon Greedy method, where the values of the coefficients are set to the values obtained in [15] for the exploration stage and [35] for the exploitation stage. This can be verified by the results shown in the MSE (Several Contamination Peaks) column of the Table 10. As in Section 5.3.3, two more situations were considered, to detect the highest peak of contamination and to generate the most accurate estimated model of lake water quality. As expected, the algorithm that best detects the highest peak is the Enhanced GP-based PSO (Exploitation). By a small difference, the second with the smallest error is the Contamination algorithm. With respect to the generation of the most reliable water quality model, the one that obtained the best result is the Enhanced GP-based PSO based on the Epsilon Greedy method, and in second place, the Enhanced GP-based PSO (Exploration). These results demonstrate that the changes of approach, exploration and then exploitation, during the experiment is the best line to solve multi-modal problems, which is the case of detecting the various peaks of contamination of the water resource.

Table 10: Comparison of the MSE and the error of the eight algorithms

Algorithm	MSE (Several Contamination Peaks)	Error (A Contamination Peak)	MSE (Model of the Lake)
Local Best	2.68687 ± 7.34544	0.89471 ± 3.19382	0.27867 ± 0.60573
Global Best	2.69164 ± 7.43596	2.36964 ± 4.20148	0.17335 ± 0.31163
Uncertainty	2.45316 ± 4.39283	2.11673 ± 3.61938	0.13680 ± 0.22764
Contamination	4.04210 ± 8.18967	0.00224 ± 0.01044	0.29742 ± 0.59782
Classic PSO	2.69269 ± 7.16223	1.73219 ± 4.00487	0.16819 ± 0.29399
Enhanced GP-based PSO (Exploration)	1.94280 ± 4.66284	1.62445 ± 3.92491	0.07465 ± 0.12707
Enhanced GP-based PSO (Exploitation)	3.80756 ± 6.56296	**0.00164** ± **0.00494**	0.21760 ± 0.42043
Epsilon Greedy Method	**1.62643** ± **3.64945**	0.00984 ± 0.03666	**0.07018** ± **0.10068**

The comparison between the eight algorithms at different distances traveled is shown in Fig. 6. To improve the visualization of the mean MSE and its 95% confidence interval at the end of the episode, Fig. 6b is shown, which is a zoom of Fig. 6a at the end of the episode (15,000 meters traveled). Throughout the episode, the three algorithms with the highest mean of MSE are the Local Best algorithm, the Contamination algorithm, and the Enhanced GP-based PSO (exploitation). This is because these three algorithms focus on exploiting the highest peak, so by not exploring the surface, they are not able to detect all the contamination peaks.

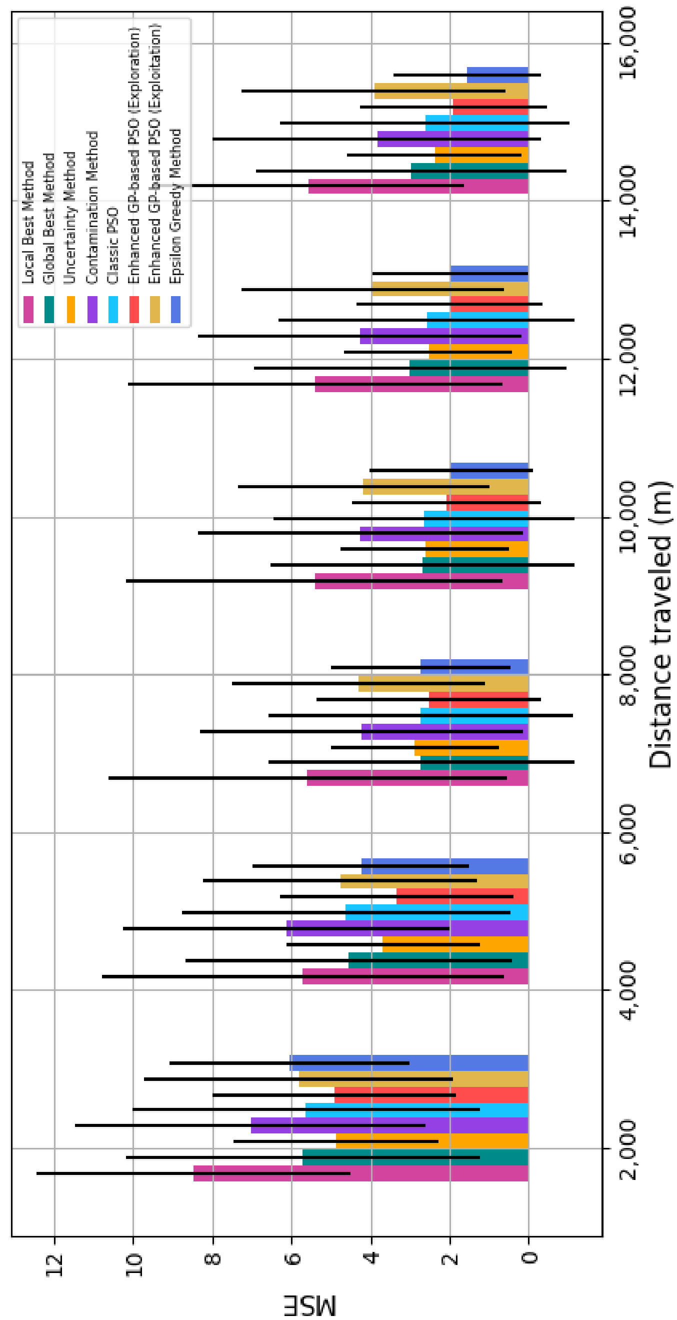
Local Best Method
Global Best Method
Uncertainty Method
Contamination Method
Classic PSO
Enhanced GP-based PSO (Exploration)
Enhanced GP-based PSO (Exploitation)
Epsilon Greedy Method
MSE
Distance traveled (m)

(a)

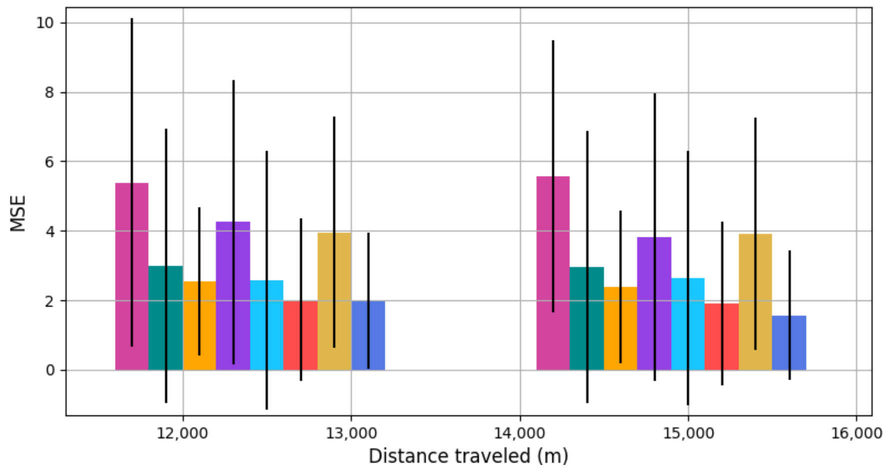

(b)

Fig. 6: Mean of the MSE and its 95% confidence interval for the detection of zones with high levels of contamination of the Local Best algorithm, the Global Best algorithm, the Uncertainty algorithm, the Contamination algorithm, the Classic PSO, the Enhanced GP-based PSO (Exploration), the Enhanced GP-based PSO (Exploitation), and the Epsilon Greedy method

Fig. 7 shows the results obtained in the experiments of the different algorithms in one of the scenarios. In the map at the top, the movement made by the vehicles and the uncertainty in the exploration of the lake are shown. The movement of each ASV is represented by a line of a different color from the others. The map at the bottom shows the estimated model of the water quality parameters.

Fig. 7a shows the results obtained with the Local Best algorithm. Since in this algorithm only the term corresponding to the best position of the ASV is kept active, the ASV focuses on exploiting the area where the samples it has taken have a high level of contamination. The disadvantage of this algorithm is that the ASVs do not explore, so if two ASVs are near a peak and both are far from a second peak, the two ASVs would go to the peak that is closer, because the water samples would have a higher value near that peak and they would not notice a second peak that is far away. As a result, the ASVs get stuck in a one of the optimum. In Fig. 7b, the ASVs movements are guided by the best position of the swarm. Because of this, all ASVs go to the same zone or peak, so they do not explore the other areas with high contamination level. The vehicle movements in Fig. 7c are guided by the maximum uncertainty term of the surrogate model. This allows the ASVs to explore the entire surface of the lake, being able to go to areas where contamination is high. However, they do not stop in those areas to exploit pollution peaks. In Fig. 7d, the term that remains active is the maximum contamination term. This allows the ASVs to exploit the zone with the highest level of contamination. However, because the ASVs do not explore the surface lake, the estimated model is not accurate, so the algorithm could have a false global maximum. In other words, the pollution maximum estimated by the algorithm is a local maximum and not a global maximum, as shown in Fig. 7d. If the estimated model is compared with the ground truth (Fig. 5), it will be seen that the global maximum of the ground truth is in the northwest of the lake but the algorithm detects that the maximum is in the west of the lake. This is because the ASVs were not able to explore the surface and there is not enough data to obtain a good estimation of the water quality model. The movement of the ASVs with the Classic PSO is shown in Fig. 7e. The ASVs learn from their own experience and from the swarm, in other words, they consider the positions they have passed through and do not consider the data of the surrogate model. Because of this, after having explored and found a peak, they focus on exploiting that peak and get stuck in that area. This result can be expected since classical PSO algorithm is not intended for multi-modal problems. For the Enhanced GP-based PSO, two cases are considered: one using the coefficient values obtained in [15] (Fig. 7f), where the objective was to obtain the most accurate model of the lake water quality, and the second case is using the coefficient values obtained in [35] (Fig. 7g), where the goal was to detect the highest pollution peak. Because in Fig. 7f, the coefficients of the global best and maximum contamination are 0, the movement of the ASVs is guided by the local best and maximum uncertainty terms. This combination allows the exploration of the lake surface because it uses the uncertainty of the surrogate model, as well as the exploitation of the zones through which the ASVs are passing, since it considers the best position of the ASVs. The local best term acts as gradient for the ASV movements. In contrast, in Fig 7g, the movement of the ASVs is mainly guided by the terms of local best and maximum contamination, the best global also has a small influence on the movements of the ASVs. Because of this, the ASVs try to reach the area where the maximum pollution peak is located and while heading to that area, they exploit the zones they pass through. However, the same case as for the Contamination algorithm can be seen with this combination of coefficient values. Since there is not enough data to estimate a good model, the ASVs go to one of the local peaks and get stuck in that area. Fig. 7h represents the results obtained by applying the Epsilon Greedy method with the values of case 3 (Section 5.3.3). At the beginning, the exploration probability is high, so they explore more lake surface while exploiting the areas they are passing through, this is due to the combination of coefficient values. As the ASVs increase the distance traveled, the exploration probability decreases and they focus more on exploiting the areas with high levels of contamination. Because the algorithm focuses more on exploration at the beginning, the surrogate model was able to generate an accurate model, so when the probability of exploitation is higher, the ASVs target the true global maximum.

Fig. 8 shows the movement of the vehicles, with the Epsilon Greedy method, during different distances traveled, as well as the evolution of the uncertainty data and the model estimated by the surrogate model. The initial points of the ASVs are represented by a black circle, and the end point at that instant is represented by a red square. Fig. 8a represents the movement of the vehicles after 1,000 meters traveled. The figure above shows how the uncertainty is high in the middle of the

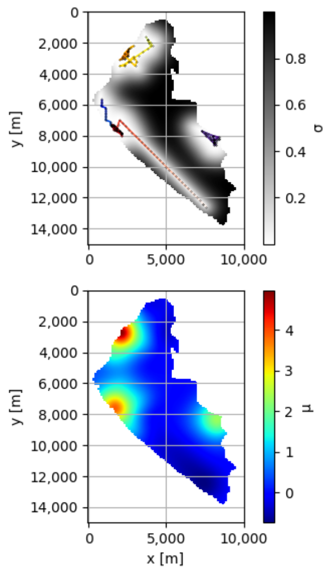

(a) Local Best algorithm

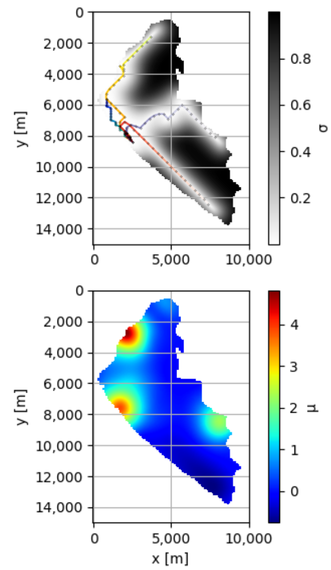

(b) Global Best algorithm

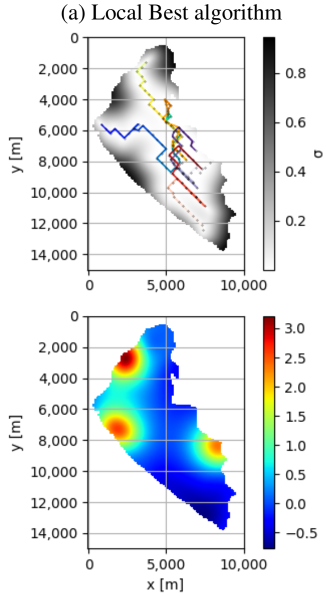

(c) Uncertainty algorithm

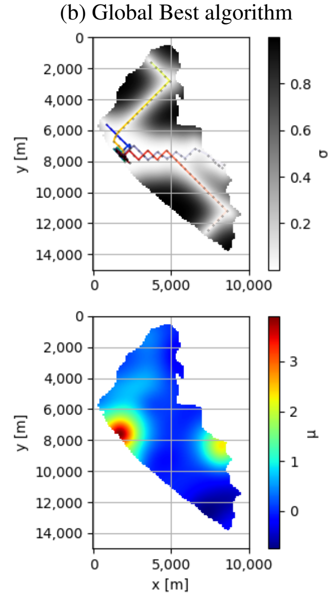

(d) Contamination algorithm

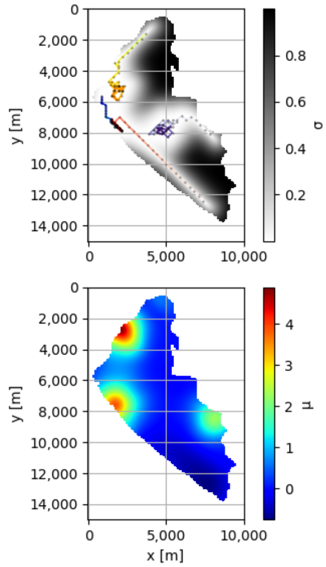

(e) Classic PSO

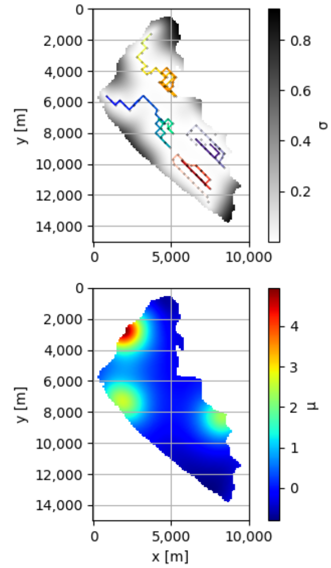

(f) Enhanced GP-based PSO (Exploration)

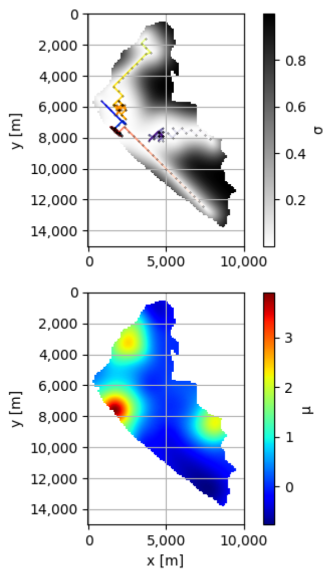

(g) Enhanced GP-based PSO (Exploitation)

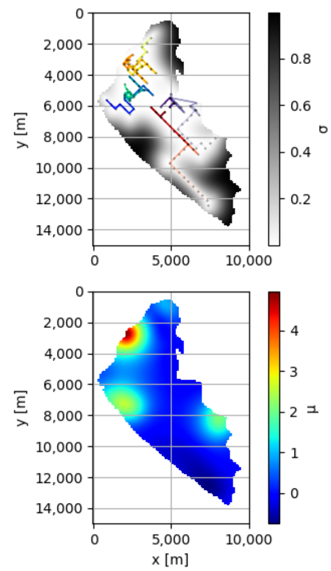

(h) Epsilon Greedy method

Fig. 7: Representation of the Ypacarai Lake monitoring system. The ASV trajectories and model uncertainty are represented in the top graphs (black and white map with coloured line traces), while the surrogate model mean is represented in the bottom graph (coloured map).

lake and the generated model estimates low values compared to the real lake model. As the vehicles move around, the uncertainty decreases and the areas of highest contamination are being better detected in the generated model as shown in Fig. 8b with 3,750 meters traveled. In Fig. 8c, the vehicles have traveled 7,500 meters, half of the episode. At that instant, the uncertainty is high in only a few sectors of the map and, with the samples taken by the vehicles, it is now possible to define the areas where pollution is high. Finally, Fig. 8d shows the end of the episode, where most of the lake was already explored and the contamination zones could be fully detected.

6 Discussion of the Results

The main findings of this work are discussed below:

- The Local Best algorithm focuses on exploiting the areas through which the ASVs pass. Because of this, if the ASVs detect a peak, they get stuck on that peak because they have no way to escape from that zone. With this algorithm, each ASVs can exploit different areas as in Fig. 7a.
- Unlike the Local Best algorithm, in the Global Best algorithm most of the surface can be explored. However, as all ASVs are guided by a single best position, the fleet targets the same peak and is not able to exploit different areas.
- The Uncertainty algorithm has the advantage that ASVs are able to explore the surface of the water resource and target unexplored areas. However, they cannot exploit areas with high levels of contamination like the Contamination algorithm.
- The advantage of the Contamination algorithm is the ability to exploit the area with the highest contamination peak, but the algorithm is not able to exploit local peaks or explore the surface.
- The Enhanced GP-based PSO with the coefficient values obtained in [15] is able to obtain an accurate water quality model of the water resource. This algorithm combines exploration of unexplored areas and exploitation of the areas through which the ASVs pass. Nonetheless, for solving multi-modal problems in the monitoring system, this algorithm obtained the second best performance, so it needs some adjustments to improve its performance.
- The Enhanced GP-based PSO with the values of the coefficients obtained in [35] has the best performance for detecting the highest contamination peak. Nevertheless, when there is more than one peak, the algorithm is not able to find all the peaks because it does not scan the surface and may get stuck on a local peak.
- The algorithm that has the best performance in detecting water resource contamination peaks is the Enhanced GP-based PSO based on the Epsilon Greedy method. This is due to the ability of the algorithm to switch approaches during the episode, between exploration and exploitation, having a high probability of exploration at the beginning and a high probability of exploitation at the end. This allows the algorithm to generate an accurate model of the lake, and then,

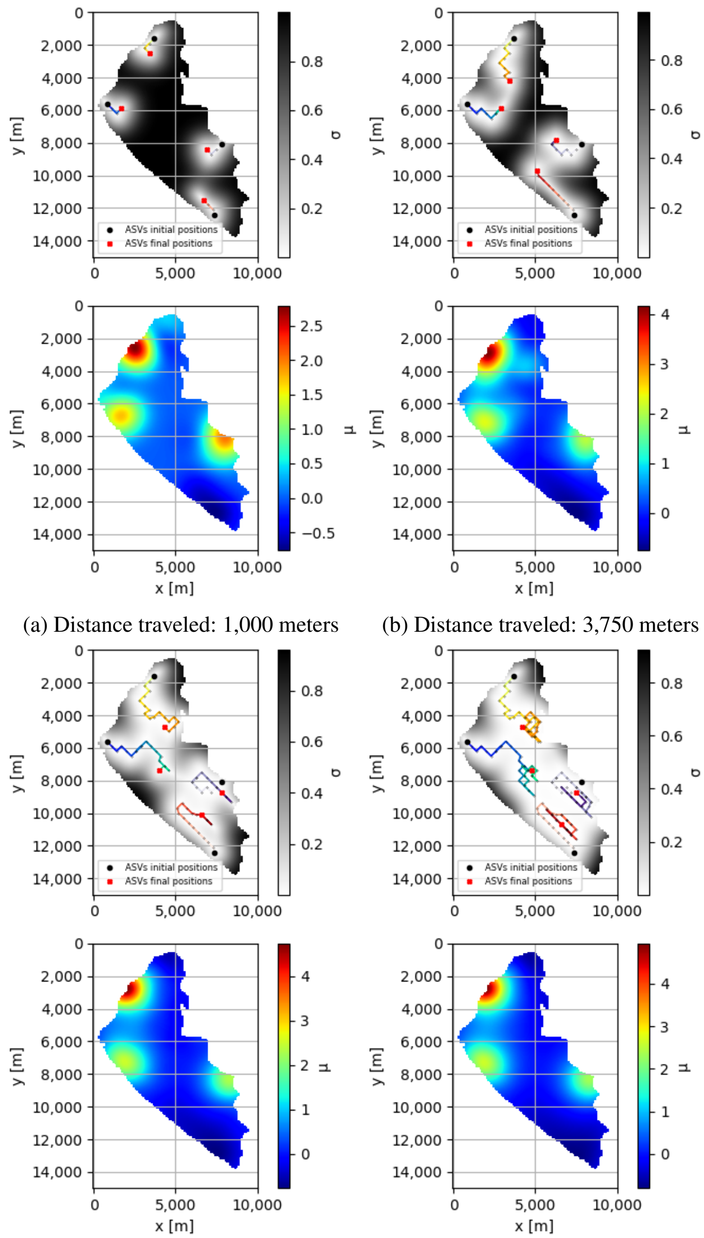

(a) Distance traveled: 1,000 meters (b) Distance traveled: 3,750 meters

(c) Distance traveled: 7,500 meters (d) Distance traveled: 15,000 meters

Fig. 8: Representation of the Ypacarai Lake monitoring system in different distances traveled. The black dots represent the initial position of the ASV, while the red square represents the final position of the ASV at that instant.

with a good model estimated, to exploit the areas where there are high levels of contamination.
- It is clear that further research is required to determine the optimal dynamic of the Enhanced GP-based PSO algorithms.

7 Conclusions

This work consisted of the simulation and comparison of different path planners based on PSO whose main objective was to detect the different peaks of contamination of a water resource. In addition to detecting the contamination zones, two other situations were analyzed, the performance of the path planners to detect the highest peak of contamination and the ability to generate a water quality model of the water resource as similar as possible to the real model or ground truth. The algorithms that were considered for comparison are: the Classic PSO; the Enhanced GP-based PSO with two different combinations of coefficients, one of them is the one obtained in [15], which focuses on exploring the surface of the water resource and obtaining an accurate model of it, and the other combination is the one obtained in [35], which focuses on exploiting the area with the highest contamination of the water resource; the Enhanced GP-based PSO based on the Epsilon Greedy method, this method allows having dynamic coefficients during the episode, due to this, the path planner can change its focus during the monitoring; and four variants of the Enhanced GP-based PSO, where in each variant the velocity term and one of the exploration (c_2 and c_3) or exploitation (c_1 and c_4) terms were left active with the objective of observing the influence of these terms in the monitoring of the zones with a high level of contamination. The results showed that the path planner that has the best performance to detect the different contamination zones and obtain the most accurate model of the water quality of the water resource is the Enhanced GP-based PSO based on the Epsilon Greedy method using the values of the coefficients obtained in [15] and [35]. The algorithm that has the best performance in finding the highest pollution peak is the Enhanced GP-based PSO with the data obtained in [35]. These results show that in order to solve multi-modal problems, such as detecting the different pollution peaks, the focus of the algorithm must change during the search process. From this, it is proposed as a future direction of research, the development of a multi-modal informative path planning based on PSO for monitoring tasks, where the focus of the algorithm will be in setting the appropriated values of the PSO coefficient according to the mission to be carried out. This is different from what is considered in the Epsilon-greedy algorithm that switch between exploration and exploitation randomly.

Acknowledgements This work has been partially funded by the regional government Junta de Andalucía under the Projects “Despliegue Inteligente de una red de Vehículos Acuáticos no Tripulados for the monitorization of Recursos Hdricos US-1257508’ and ’Despliegue y Control of a red Inteligente of Vehculos Autónomos Acuáticos for the monitorisation of Recursos Hdricos Andaluces PY18-RE0009'.

References

1. Arzamendia M, Espartza I, Reina DG, Toral S, Gregor D (2019) Comparison of eulerian and hamiltonian circuits for evolutionary-based path planning of an autonomous surface vehicle for monitoring ypacarai lake. Journal of Ambient Intelligence and Humanized Computing 10(4):1495–1507
2. Arzamendia M, Gregor D, Reina DG, Toral SL (2019) An evolutionary approach to constrained path planning of an autonomous surface vehicle for maximizing the covered area of ypacarai lake. Soft Computing 23(5):1723–1734
3. Arzamendia M, Reina DG, Toral S, Gregor D, Asimakopoulou E, Bessis N (2019) Intelligent online learning strategy for an autonomous surface vehicle in lake environments using evolutionary computation. IEEE Intelligent Transportation Systems Magazine 11(4):110–125
4. Birattari M, Kacprzyk J (2009) Tuning metaheuristics: a machine learning perspective, vol 197. Springer
5. Blanchard A, Sapsis T (2020) Informative path planning for anomaly detection in environment exploration and monitoring. arXiv preprint arXiv:200510040
6. Bottarelli L, Bicego M, Blum J, Farinelli A (2019) Orienteering-based informative path planning for environmental monitoring. Engineering Applications of Artificial Intelligence 77:46–58
7. Cf O (2015) Transforming our world: the 2030 agenda for sustainable development. United Nations: New York, NY, USA
8. Cui Y, Zhong J, Yang F, Li S, Li P (2020) Multi-subdomain grouping-based particle swarm optimization for the traveling salesman problem. IEEE Access 8:227,497–227,510
9. Dirección General del Centro Multidisciplinario de Investigaciones Tecnológicas (CEMIT) (2018) Servicios de monitoreo de calidad de agua por campañas de muestreo en el lago ypacaraí. 2016 -2018. Tech. rep., Universidad Nacional de Asunción (UNA)
10. Dirección General del Centro Multidisciplinario de Investigaciones Tecnológicas (CEMIT) (2021) Monitoreo de calidad de agua por campañas de muestreo en el lago ypacaraí 2019 - 2021. Tech. rep., Universidad Nacional de Asunción (UNA)
11. Duan H, Loiselle SA, Zhu L, Feng L, Zhang Y, Ma R (2015) Distribution and incidence of algal blooms in lake taihu. Aquatic Sciences 77(1):9–16
12. Feurer M, Hutter F (2019) Hyperparameter optimization. In: Automated Machine Learning, Springer, Cham, pp 3–33
13. Gul F, Rahiman W, Alhady S, Ali A, Mir I, Jalil A (2021) Meta-heuristic approach for solving multi-objective path planning for autonomous guided robot

using pso–gwo optimization algorithm with evolutionary programming. Journal of Ambient Intelligence and Humanized Computing 12(7):7873–7890

14. Guo B, Hu J, Wu W, Peng Q, Wu F (2019) The tabu_genetic algorithm: a novel method for hyper-parameter optimization of learning algorithms. Electronics 8(5):579
15. Jara Ten Kathen M, Jurado Flores I, Gutierrez Reina D (2022) A comparison of pso-based informative path planners for autonomous surface vehicles for water resource monitoring. In: 2022 7th International Conference on Machine Learning Technologies (ICMLT), pp 271–276
16. Kennedy J, Eberhart R (1995) Particle swarm optimization. In: Proceedings of ICNN'95-international conference on neural networks, IEEE, vol 4, pp 1942–1948
17. Kim Y, Chung M (2019) An approach to hyperparameter optimization for the objective function in machine learning. Electronics 8(11):1267
18. Kushner HJ (1964) A new method of locating the maximum point of an arbitrary multipeak curve in the presence of noise
19. Lessmann S, Caserta M, Arango IM (2011) Tuning metaheuristics: A data mining based approach for particle swarm optimization. Expert Systems with Applications 38(10):12,826–12,838
20. López Moreira GA, Hinegk L, Salvadore A, Zolezzi G, Hölker F, Monte Domecq S RA, Bocci M, Carrer S, De Nat L, Escribá J, et al (2018) Eutrophication, research and management history of the shallow ypacaraí lake (paraguay). Sustainability 10(7):2426
21. Marini F, Walczak B (2015) Particle swarm optimization (pso). a tutorial. Chemometrics and Intelligent Laboratory Systems 149:153–165
22. Michalak AM, Anderson EJ, Beletsky D, Boland S, Bosch NS, Bridgeman TB, Chaffin JD, Cho K, Confesor R, Daloğlu I, et al (2013) Record-setting algal bloom in lake erie caused by agricultural and meteorological trends consistent with expected future conditions. Proceedings of the National Academy of Sciences 110(16):6448–6452
23. Mockus J, Tiesis V, Zilinskas A (1978) The application of Bayesian methods for seeking the extremum. Towards Global Optimization 2(117-129):2
24. Peralta F, Arzamendia M, Gregor D, Reina DG, Toral S (2020) A comparison of local path planning techniques of autonomous surface vehicles for monitoring applications: The ypacarai lake case-study. Sensors 20(5):1488
25. Peralta F, Reina DG, Toral S, Arzamendia M, Gregor D (2021) A bayesian optimization approach for multi-function estimation for environmental monitoring using an autonomous surface vehicle: Ypacarai lake case study. Electronics 10(8):963
26. Peralta F, Reina DG, Toral S, Arzamendia M, Gregor D (2021) A bayesian optimization approach for water resources monitoring through an autonomous surface vehicle: The ypacarai lake case study. IEEE Access 9:9163–9179, DOI 10.1109/ACCESS.2021.3050934
27. Peralta F, Yanes S, Reina DG, Toral S (2021) Monitoring water resources through a bayesian optimization-based approach using multiple surface vehi-

cles: The ypacarai lake case study. In: 2021 IEEE Congress on Evolutionary Computation (CEC), IEEE, pp 1511–1518
28. Rasmussen CE (2003) Gaussian processes in machine learning. In: Summer school on machine learning, Springer, pp 63–71
29. Ratnaweera A, Halgamuge SK, Watson HC (2004) Self-organizing hierarchical particle swarm optimizer with time-varying acceleration coefficients. IEEE Transactions on Evolutionary Computation 8(3):240–255, DOI 10.1109/TEVC.2004.826071
30. Roman I, Ceberio J, Mendiburu A, Lozano JA (2016) Bayesian optimization for parameter tuning in evolutionary algorithms. In: 2016 IEEE Congress on Evolutionary Computation (CEC), IEEE, pp 4839–4845
31. Sánchez-García J, Reina DG, Toral S (2019) A distributed pso-based exploration algorithm for a uav network assisting a disaster scenario. Future Generation Computer Systems 90:129–148
32. Senthil Arumugam M, Rao M, Chandramohan A (2008) A new and improved version of particle swarm optimization algorithm with global-local best parameters. Knowl Inf Syst 16:331–357, DOI 10.1007/s10115-007-0109-z
33. Srinivas N, Krause A, Kakade SM, Seeger M (2009) Gaussian process optimization in the bandit setting: No regret and experimental design. arXiv preprint arXiv:09123995
34. Ten Kathen MJ, Flores IJ, Reina DG (2021) An informative path planner for a swarm of asvs based on an enhanced pso with gaussian surrogate model components intended for water monitoring applications. Electronics 10(13):1605
35. Ten Kathen MJ, Reina DG, Flores IJ (2022) A comparison of pso-based informative path planners for detecting pollution peaks of the ypacarai lake with autonomous surface vehicles. In: International Conference on Optimization and Learning OLA'2022
36. Williams C, Rasmussen C (2006) Gaussian processes for machine learning, vol 2. MIT press Cambridge, MA
37. Wu J, Chen XY, Zhang H, Xiong LD, Lei H, Deng SH (2019) Hyperparameter optimization for machine learning models based on bayesian optimization. Journal of Electronic Science and Technology 17(1):26–40
38. Xin J, Li S, Sheng J, Zhang Y, Cui Y (2019) Application of improved particle swarm optimization for navigation of unmanned surface vehicles. Sensors 19(14):3096
39. Xu H, Paerl HW, Qin B, Zhu G, Gaoa G (2010) Nitrogen and phosphorus inputs control phytoplankton growth in eutrophic lake taihu, china. Limnology and oceanography 55(1):420–432
40. Yanes S, Reina DG, Toral S (2020) A deep reinforcement learning approach for the patrolling problem of water resources through autonomous surface vehicles: The ypacarai lake case. IEEE Access 8:204,076–204,093
41. Yanes S, Peralta F, Reina DG, Toral S (2021) A sample-efficiency comparison between evolutionary algorithms and deep reinforcement learning for path planning in an environmental patrolling mission. In: 2021 IEEE Congress on Evolutionary Computation (CEC), IEEE, pp 71–78

42. Yanes S, Reina DG, Toral S (2021) A dimensional comparison between evolutionary algorithm and deep reinforcement learning methodologies for autonomous surface vehicles with water quality sensors. Sensors 21(8):2862
43. Yanes S, Reina DG, Toral S (2021) A multiagent deep reinforcement learning approach for path planning in autonomous surface vehicles: The ypacarac-lake patrolling case. IEEE Access
44. Yanes S, Peralta F, Córdoba AT, del Nozal ÁR, Marín ST, Reina DG (2022) An evolutionary multi-objective path planning of a fleet of asvs for patrolling water resources. Engineering Applications of Artificial Intelligence 112:104,852